Received: 17 August 2022 | Revised: 14 October 2022 | Accepted: 21 October 2022

DOI: 10.1096/fj.202201339R

THE FASEB JOURNAL

RESEARCH ARTICLE

Magnesium homeostasis in deoxygenated sickle erythrocytes is modulated by endothelin-1 via Na^+/Mg^{2+} exchange

José R. Romero[1] | **Yaritza Inostroza-Nieves**[1,2] | **Patricia Pulido-Perez**[1] | **Pablo Lopez**[1] | **Jay G. Wohlgemuth**[3] | **Jeffrey S. Dlott**[3] | **L. Michael Snyder**[3] | **Seth L. Alper**[4] | **Alicia Rivera**[4,5]

[1]Division of Endocrinology, Diabetes and Hypertension, Brigham and Women's Hospital, and Department of Medicine, Harvard Medical School, Boston, Massachusetts, USA

[2]Department of Biochemistry and Pharmacology, San Juan Bautista School of Medicine, Caguas, Puerto Rico, USA

[3]Quest Diagnostics, Secaucus, New Jersey, USA

[4]Division of Nephrology and Vascular Biology Research Center, Beth Israel Deaconess Medical Center, and Department of Medicine, Harvard Medical School, Boston, Massachusetts, USA

[5]Division of Laboratory Medicine, Boston Children's Hospital, and Department of Pathology, Harvard Medical School, Boston, Massachusetts, USA

Correspondence
Alicia Rivera, Beth Israel Deaconess Medical Center, 99 Brookline Ave. Building RN 380A, Boston, MA 02215, USA.
Email: arivera3@bidmc.harvard.edu

Funding information
National Heart, Lung, and Blood Institute, Grant/Award Number: HL67699, HL090632 and HL096518; National Institute of Diabetes and Digestive and Kidney Diseases, Grant/Award Number: DK064841; Quest Diagnostics

Abstract

Painful crises in sickle cell disease (SCD) are associated with increased plasma cytokines levels, including endothelin-1 (ET-1). Reduced red cell magnesium content, mediated in part by increased Na^+/Mg^{2+} exchanger (NME) activity, contributes to erythrocyte K^+ loss, dehydration and sickling in SCD. However, the relationship between ET-1 and the NME in SCD has remained unexamined. We observed increased NME activity in sickle red cells incubated in the presence of 500 nM ET-1. Deoxygenation of sickle red cells, in contrast, led to decreased red cell NME activity and cellular dehydration that was reversed by the NME inhibitor, imipramine. Increased NME activity in sickle red cells was significantly blocked by pre-incubation with 100 nM BQ788, a selective blocker of ET-1 type B receptors. These results suggest an important role for ET-1 and for cellular magnesium homeostasis in SCD. Consistent with these results, we observed increased NME activity in sickle red cells of three mouse models of sickle cell disease greater than that in red cells of C57BL/J6 mice. In vivo treatment of BERK sickle transgenic mice with ET-1 receptor antagonists reduced red cell NME activity.

Abbreviations: AA, normal hemoglobin A red cell; CK2, casein kinase II; CTL, control; CWS-Mg, choline washing solution; ET-1, endothelin-1; ETRA/B, endothelin-1 receptors antagonists; ETRB, endothelin-1 receptor B; HIF-1, hypoxia inducible factor-1; IMP, imipramine; MCV, mean cellualr volume; NME, Na^+/Mg^{2+} exchanger; PAF, platelet activator factor; PGE2, prostaglandins E2; PKC, protein kinase C; PMSF, phenylmethylsulfonyl fluoride; RANTES, regulated upon activation normal T cell expressed and presumably secreted; SCD, sickle cell disease; SEM, standard error of mean; SS, hemoglobin S red cells; TRPM, transient receptor potential melastatin.

Our results suggest that ET-1 receptor blockade may be a promising therapeutic approach to control erythrocyte volume and magnesium homeostasis in SCD and may thus attenuate or retard the associated chronic inflammatory and vascular complications of SCD.

1 | INTRODUCTION

Among patients with sickle cell disease (SCD), 5% experience 3–10 potentially lethal vaso-occlusive painful crises annually.[1,2] Vaso-occlusive crises are initiated, in part, by red cell deoxygenation and by elevated plasma levels of cytokines such as endothelin-1 (ET-1), leading to increased adhesive interactions among sickle red cells, between sickle red cells and endothelium and involving plasma factors, through mechanisms that remain incompletely understood.[3–6] ET-1 plays important roles in the disordered erythrocyte homeostasis, inflammation, vaso-occlusion, tissue injury, and pain common to the pathophysiology of SCD.[7,8] ET-1 levels are increased in SCD,[9,10] and in vivo treatment with ET-1 receptor antagonists improve hematological parameters and reduced oxidant stress in mouse models of SCD.[11] However, the mechanisms by which ET-1 receptor antagonists mediate their beneficial effects in SCD remain unclear.

Dysregulated Mg^{2+} levels have been reported in SCD and in patients with Type 2 diabetes,[12,13] hypertension, and stroke, all diseases with an important inflammatory component.[14–16] Low Mg^{2+} levels are accompanied by oxidant stress, impaired vascular function and increased inflammation, all associated with the pathophysiology of SCD.[17,18] Low cellular Mg^{2+} levels stimulate cytokine production in and release from endothelial cells and modulate activity of NF-κB, a master regulator of cytokine production.[19,20] Intracellular Mg^{2+} regulates multiple additional activities linked to SCD, including casein kinase II (CK2),[21] PKC[22–24] and hypoxia-inducible factor-1 (HIF-1).[25] Thus, regulation of Mg^{2+} levels has been proposed as a therapeutic target in SCD.[26–28] A preliminary study reported that the activity of the Na^+/Mg^{2+} exchanger (NME) in sickle erythrocytes was significantly reduced after 6 months of dietary Mg^{2+} supplementation in SCD patients.[29] This decrease was accompanied by a significant increase in intracellular Mg^{2+} content and by a decrease in erythroid K/Cl cotransport in 17 SCD patients. Similar results were observed in the SAD mouse model of SCD, in which dietary Mg^{2+} supplementation increased erythrocyte Mg^{2+} content by up to 70%,[30] while reducing both erythrocyte density and K/Cl cotransporter activity by 50%. However, a phase I clinical trial of 6 months duration to evaluate dietary Mg^{2+} as an adjuvant to hydroxyurea treatment of SCD revealed no significant differences in red cell Mg^{2+} concentration or NME activity, while nonetheless reducing erythroid K/Cl cotransport activity.[31]

Cellular Mg^{2+} homeostasis is regulated by extracellular Mg^{2+} influx mediated by a subset of Transient Receptor Potential Melastatin subfamily (TRPM) channels including TRPM2 and TRPM7,[32] and Mg^{2+} efflux mediated by SLC41A1,[33,34] variously reported to mediate NME activity[35] or Na^+-independent Mg^{2+} efflux.[34] Variations in Mg^{2+} levels regulate transport processes that control the ionic composition and volume of many cell types. Cellular Mg^{2+} content is heavily dependent on concentrations of Mg^{2+}-binding metabolites (with ATP and 2,3-bisphosphoglycerate being the major Mg^{2+} buffers), on intracellular pH, and intracellular pO_2. NME activity imports Na^+ into the cell down its electrochemical gradient in exchange for energetically uphill efflux of intracellular Mg^{2+}.[36,37] NME activity is blocked by the removal of external Na^+ or by intracellular ATP depletion and can be partially inhibited to varying degrees by amiloride,[38] quinidine,[39] and tricyclic antidepressants such as imipramine.[40] Despite their poor specificity, quinidine and imipramine have been used extensively to characterize NME activity independent of Ca^{2+} transporters. We have previously reported on increased NME activity and reduced intracellular Mg^{2+} levels in human sickle erythrocytes.[41] However, physiological modulators of NME in sickle erythrocytes remain little investigated. We postulate that ET-1 regulates cellular Mg^{2+} via NME which leads to cellular dehydration in sickle erythrocytes. Here, we investigate the role of ET-1 on NME activity in and sickle erythrocytes and the contribution of this regulation to red cell hydration status.

2 | MATERIALS AND METHODS

2.1 | Drugs and chemicals

A23187 ionophore was purchased from Calbiochem (La Jolla, CA, USA). Bovine serum albumin was from Roche (Indiana, IN, USA). Endothelin-1, Platelet Activator Factor (PAF), RANTES, and all other reagents were from Sigma-Aldrich (St Louis, MO, USA).

2.2 | Human blood samples

Blood from sickle cell disease patients were collected after signed informed consent, following approval by the Boston Children's Hospital Institutional Review Board, and in

compliance with the U.S. Health Insurance Portability and Accountability Act (HIPAA) regulations.

2.3 | Preparation of erythrocytes

Whole blood collected in heparinized tubes was passed through cotton to deplete leukocytes and centrifuged in a Sorvall RC28S (Newtown, CT, USA) at 3000 rpm for 4 min at 4°C as previously described.[41] The plasma was removed by aspiration, and erythrocytes were washed 4 times with ice-cold Mg^{2+}-free Choline Wash Solution (CWS-Mg-free) containing 150 mM Choline Cl, 10 mM Tris MOPS (3-[N-Morpholino]propanesulphonic acid), pH 7.4 (4°C) and 20 mM Sucrose (299–310 mOsm) as determined by freezing point osmometry (Osmette A, Precision Systems, MA). A 50% cell suspension was made in CWS-Mg free, and Manual hematocrit and mean cellular volume (MCV) were measured using the ADVIA 120 autoanalyzer (Bayer Siemans, Washington DC, USA). Aliquots of this 50% suspension were diluted with 0.02% Acationox in double-distilled water to measure intracellular Na^+, K^+, and Mg^{2+} contents by atomic absorption spectrophotometry (Perkin Elmer 800, Waltham, MA, USA).

2.4 | Animals

BERK mice carry a hemizygous human transgenic insertion containing normal human α-, γ-, and δ-globins and human sickle β-globin, in a mouse genetic background with targeted deletion of murine α- and β-globins ($\alpha^{-/-}$, $\beta^{-/-}$, Tg). BERK mice have severe disease that partially phenocopies human sickle cell anemia (hemolysis, reticulocytosis, anemia, extensive organ damage, and shortened life span) and exhibit high levels of oxidative stress.[42] Our mouse colony was generated by breeding $\alpha^{-/-}$, $\beta^{-/-}$, Tg males with $\alpha^{-/-}$, $\beta^{+/-}$, Tg females. BERK and BERK-trait mice (homozygous α knockout, heterozygous β knockout) of both sexes were studied at ages of 3–6 months. HbC ($Hba^+/Hba^+/Hbb^0/Hbb^0$) transgenic mice[43] and NY1DD transgenic mice[44] were provided by Dr. Mary Fabry (Albert Einstein College of Medicine, Bronx, NY, USA). Male and female mice between 8 and 16 weeks of age were studied. SAD mice carried the human β_S (β6Val), β_S-Antilles (β23Ile), and D-Punjab (β121Glu) globin β-chain transgene on C57Bl/6J backgrounds, and were from the Alper lab colony at Beth Israel Deaconess Medical Center (derived from animals originally provided by Dr. Marie Trudel, IRCM, Montreal, Canada).[45] Male SAD mice aged 8–10 months were studied. All our wild-type animals were C57Bl/6J from Jackson Laboratories (The Jackson Laboratory, Bar Harbor, ME). All procedures for study, animal care, and euthanasia followed approval by the Boston Children's Hospital Animal Care and Use Committees.

2.5 | ADVIA hematological parameters

Blood cell counts were determined by ADVIA automated hematology analyzer (Bayer Diagnostics, Tarrytown, NY, USA). Freshly isolated whole blood human or mouse was collected in heparinized tubes, and an aliquot of 250 µl was used to perform the erythrocyte and reticulocyte counts and white blood differential for each sample using software programs specific for mouse or human blood.

2.6 | Determination of Na^+/Mg^{2+} exchange (NME) activity

Erythrocytes at 10% hematocrit were Mg^{2+}-loaded for 30 min at 37°C in the presence of 6 µM A23187. The Mg^{2+} loading solution contained (in mM): 140 KCl, 12 $MgCl_2$, 10 Glucose, and 10 Tris MOPS, pH 7.4 (37°C). The osmolarity was balanced with sucrose to approximately ~300 mOsm. A23187 was subsequently removed by four consecutive washes using 0.1% BSA at 37°C. The cells were further washed 4 times with Mg-free CWS at 4°C to remove extracellular Mg^{2+}. A 50% cell suspension was made in Mg^{2+}-free CWS. Sodium, potassium, and magnesium cellular content were determined as described above. The NME activity assay was initiated by the addition of an aliquot of 50% cell suspension to either 6 ml NaCl or Choline Cl flux media containing (in mM): 140 NaCl or 140 Choline Cl, 10 Glucose, 10 Tris MOPS, pH 7.4 (37°C), 0.1 ouabain and 0.01 bumetanide. Triplicate samples were removed at 5 and 45 min and quickly centrifuged at 4°C. Supernatants were carefully aspirated and quickly transferred to 4 ml plastic tubes. NME activity was also measured in the presence or absence of 100 nM PAF, 100 nM PGE2, or 40 ng/ml RANTES, each added at the start of fluxes. Supernatant Mg^{2+} concentrations were determined by atomic absorption. Mg^{2+} efflux was calculated from the slope of the linear regression of total Mg^{2+} content versus time and expressed in units of mmol/L cell × h. NME activity was calculated as the difference between Mg^{2+} efflux in NaCl and in Choline Cl flux media, and MCV-corrected values were expressed as mmol/10^{13} cells × h.

2.7 | Phthalate density profile

Density distribution curves were obtained using phthalate esters in microhematocrit tubes as previously described in detail by Kurantsin-Mills et al.[46,47] Briefly, phthalate solutions were prepared to give a range of densities between 1.08 and

1.11 g/ml. The hematocrit tubes were filled with 30 µl whole blood or cell suspension and 10 µl each of different phthalate solutions of varied densities. Tubes were centrifuged at 12200 rpm for 10 min at room temperature in a temperature-controlled microcentrifuge. The number of dense cells was calculated from the total cell content below the oil layer (lower layer) divided by the total amount of cells and expressed as a percentage, as we have previously described.[48] The data are presented as percentages of dense cells versus phthalate oil densities, with connection of data points unless otherwise stated. Best-fit sigmoidal curve analysis (SigmaPlot 9.0 graphic software for Windows, Palo Alto, CA, USA) for each individual experimental curve at each condition was used to assess statistical differences between or among treatments. Values of the phthalate oil density dividing the cell population into two equal parts (D_{50}) were used to determine shifts in the cellular density profiles of red cell populations.

2.8 | Cyclic deoxygenation-oxygenation experiments in vitro

Freshly isolated human erythrocytes were incubated in a plasma-like buffer containing (in mM) 145 NaCl, 2 KCl, 25 $NaHCO_3$, 10 glucose, 0.06 adenosine, 0.04 inosine, 0.15 $MgCl_2$, 2 $CaCl_2$ and 10 µM clotrimazole for 3 h (30% hematocrit) under a 10-min oxygenation-deoxygenation cycle (ChronTrol Corp. San Diego, CA, USA). Each cycle provided 3 min of 15% O_2-5% CO_2 balanced with N_2 and 7 min of 5% CO_2 balanced with N_2 gas. The gases were humidified by bubbling in a column of isotonic saline solution at 37°C. Cell suspension aliquots were transferred to an ice bath at predetermined time points. Aliquots were taken at different time points to monitor gas levels during the 10-min cycles using a Co-oximeter (Ciba-Corning model 845, Medfield, MA, USA), as previously described.[11]

2.9 | Treatment of mice with ET-1 receptor A and B antagonists

Transgenic BERK sickle cell mice were divided into two groups of five animals per group and underwent daily intraperitoneal injections of 0.1 ml volume for 14 days (Scheme 1). ET-1 antagonists (BQ123 + BQ788) were diluted in sterile normal saline. Group A BERK mice received sterile saline (100 µl) alone. Group B mice received a mixture of BQ-123 (0.2 mg/ml stock) and BQ-788 (0.2 mg/ml stock) in 100 µl. At day 15, mice were euthanized, and blood (~1 ml) was immediately collected into ice-cold heparinized tubes for further analysis.

2.10 | ET-1 determination by HPLC

Steady state plasma levels of ET-1 were measured as described previously, with modifications.[49] Whole blood samples from mice of the strains C57Bl/6j, CD-1, SAD, BERK, NY1DD, and HbC were collected following approved IRB protocols. Animals were housed in the animal facility for two weeks after transport to avoid stress-induced cytokine production. Whole blood samples were gently mixed in microfuge tubes containing 10 mg/ml EDTA, 34.8 µg/ml PMSF, and 2 µg/ml aprotinin, then centrifuged at 2500 rpm for 10 min. 300 µl of plasma fraction was removed and transferred to a 4 ml glass tube. 600 µl ice-cold acetone mix (40 parts acetone: 1 part 1 N HCl: 5 parts double-distilled water) was added to deproteinize the sample. Deproteinized samples were incubated for 5 min on ice, and centrifuged 10 min at 3000 rpm. Supernatants were transferred to fresh glass tubes and placed in a Nitrogen evaporator to remove ≤1/3 of the sample volume (Zymark TurboVap LV, East Lyme, CT, USA). Following repeat deproteination, the resulting supernatant was dried under nitrogen, reconstituted in 75 µl of mix A (30% acetonitrile in 0.1% Trifluoracetic acid, TFA), and transferred to HPLC vials for analysis.

2.11 | HPLC unit

The SupelCosil LC-318 reverse–phase column (25 cm length, 4.6 mm id, 5 µm particle size, 300 Å) was from Supelco (Oakville, ON, USA). The RF551 fluorescence detector and temperature control chamber were from Shimadzu (Marlborough, MA, USA). ET-1 was resolved

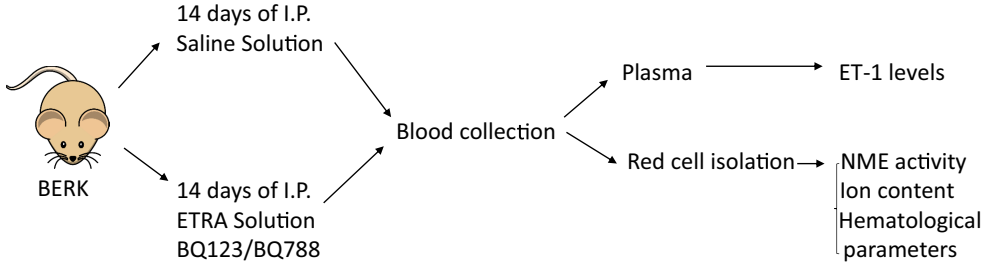

SCHEME 1 In vivo protocol for ETRA testing in sickle cell mouse model, BERK.

by gradient elution using two solvents. Mix A consisted of 30% acetonitrile in 0.1% TFA, and Mix B included 90% acetonitrile in 0.1% TFA. The injection volume was 20 μl with the mobile phase set for 1 ml/min.

2.12 | Statistics

Data are presented as mean values ± SEM. *p*-Values <.05 were considered significant. Wilcoxon rank or Mann–Whitney non-parametric tests were performed as indicated for non-normal distributed data.

3 | RESULTS

3.1 | Na^+/Mg^{2+} exchange is modulated by endothelin-1 via endothein-1 receptor B

We previously reported that human SCD erythrocytes exhibit higher rates of NME activity than normal AA erythrocytes.[41] SCD erythrocytes also have reduced intracellular Mg^{2+} content that can be modulated by increased dietary Mg^{2+}.[29] These findings are consistent with the elevated Mg^{2+} efflux activity of SCD erythrocytes. Here, we found that Na^+-induced Mg^{2+} efflux was elevated in Mg^{2+}-loaded human SCD erythrocytes as compared to normal (AA) cells (Figures 1A,B). In normal human erythrocytes, 500 nM ET-1 significantly enhances Mg^{2+} efflux in the presence of extracellular Na^+, in a manner sensitive to inhibition by an endothelin receptor B antagonist. This pattern was observed also in SCD erythrocytes, although the proportionally lower degree of activation suggested that NME in baseline conditions may be near-maximally activated. Figure 2 shows the NME activity in normal human AA and human SCD erythrocytes. We found NME activity to be enhanced 2.9-fold in SCD red cells vs. AA cells. 500 nM ET-1 enhanced NME activity 2.3-fold in normal AA red cells, whereas in SCD erythrocytes ET-1 enhanced NME by only 26% from its baseline elevated state. We also observed that 1 μM endothelin receptor B (ETRB) antagonist significantly reduced these stimulations (Figure 2).

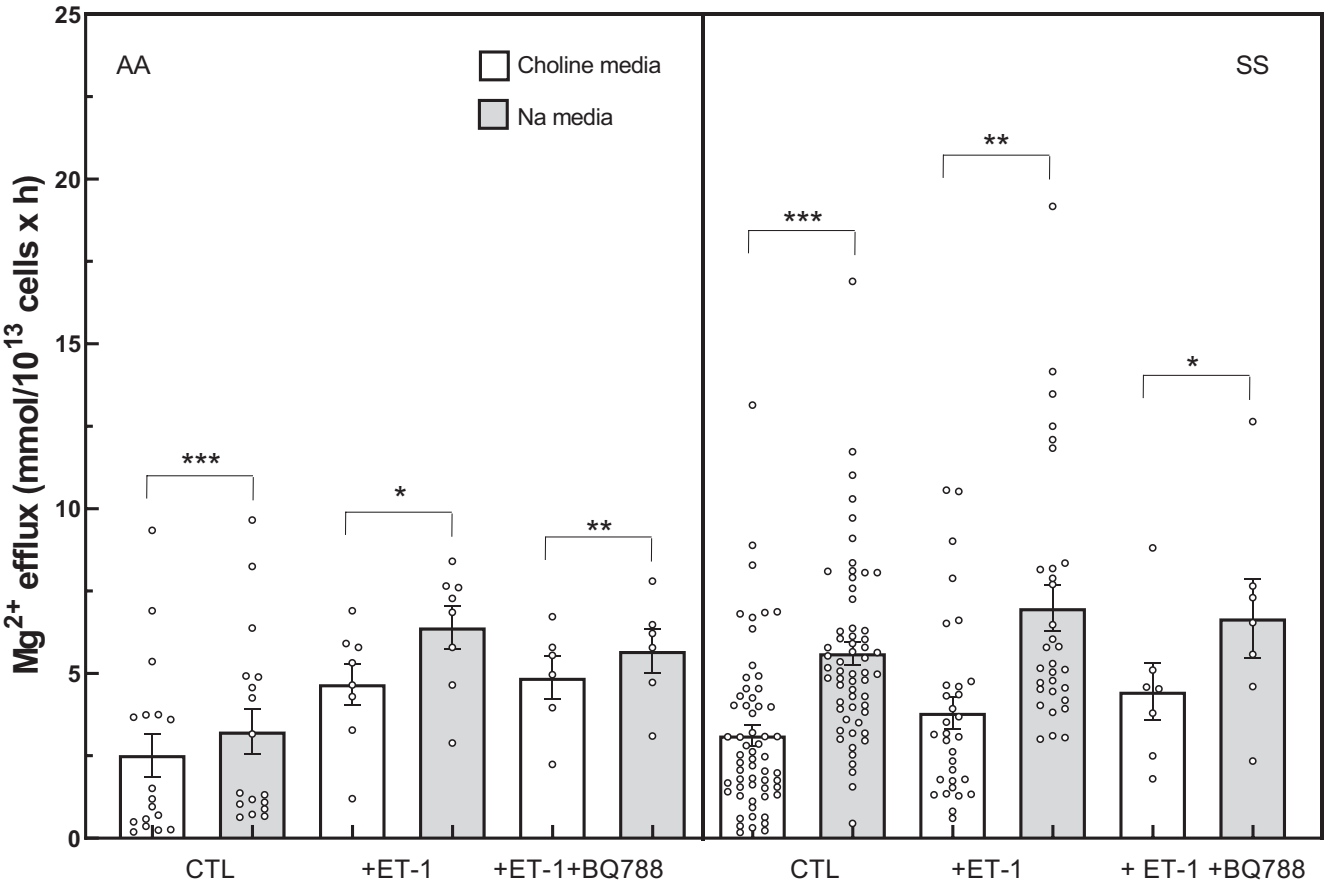

FIGURE 1 Mg^{2+} efflux in Na^+-containing and Choline-containing media. Normal and sickle erythrocytes were Mg-loaded as in *Methods*, and Mg^{2+} efflux was measured in the absence (open bars) or presence of extracellular Na^+ (gray bars). Post-loading $[Mg]_i$ was 11.86 ± 0.49 mmol/Kg Hb. Open circles represent individual triplicate experiments. Bars represent means ± SEM of >6 triplicate experiments. *$p < .01$; **$p < .002$; ***$p < .0001$ vs. corresponding choline data. Wilcoxon rank test for paired matched data, with Holm-Sidak correction for multiple comparisons.

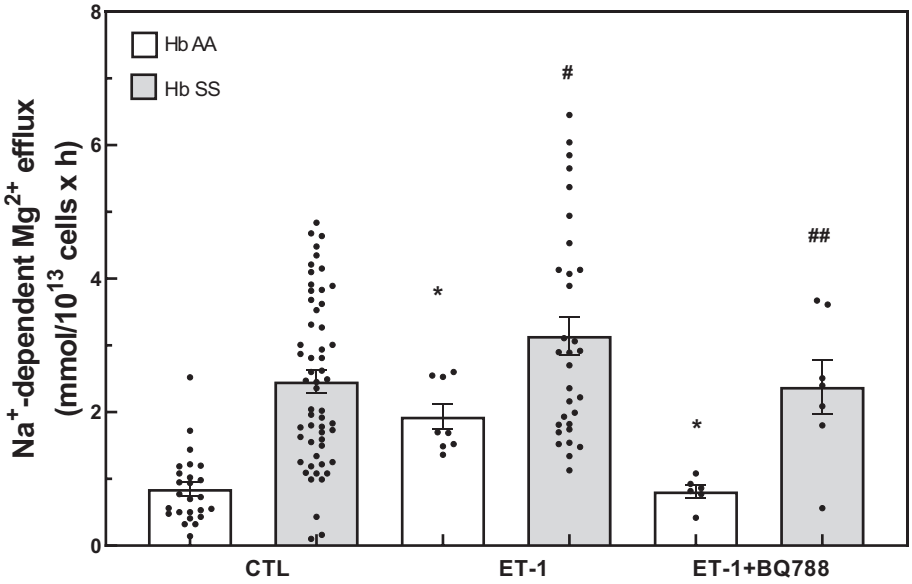

FIGURE 2 ET-1 stimulated Na^+/Mg^{2+} exchange (NME) activity in normal and sickle erythrocytes. Mg^{2+} efflux from AA (open bars) and SS red cells (gray bars) was measured as described above, and Na^+/Mg^{2+} exchange activity was estimated from the difference between Mg flux in the presence and absence of extracellular Na^+. Fluxes were normalized to MCV in each experiment. Data are means ± SEM of triplicate determinations. $^*p = .007$; $^{\#}p = .04$, $^{\#\#}p = .031$, each vs. corresponding control data (CTL). Mann–Whitney test.

The data suggest that ET-1 regulates NME via ETRB in both AA and SS (SCD) red cells. NME activity is elevated in SCD erythrocytes but retains proportionately reduced ETRB-mediated ET-1 sensitivity.

3.2 | ETRB antagonist partially reverses the ET-1 inhibitory effect on deoxygenation-stimulated SCD red cells

The contribution of NME activity to cellular Mg^{2+} regulation has not been explored in conditions of cycling deoxygenation. Figure 3A shows that Mg^{2+} efflux from non-loaded SCD red cells after cycling deoxygenation was significantly elevated in the presence of Na^+ ($p = .0001$). Incubation of SCD erythrocytes with 500 nM ET-1 under cycling deoxygenation conditions abolished the Na^+-dependent fraction of Mg^{2+} efflux (Figure 3A) without changing the Na^+-independent component of Mg^{2+} efflux (into Choline media). This effect was partially reversed by 1 μM ETRB antagonist, BQ788. To confirm the role of NME activity in this effect of BQ788, we tested imipramine, a well-known non-specific NME inhibitor in various cell types.[37,40,50] We observed that 100 μM imipramine completely blocked the NME-inhibitory effect of ET-1 in conditions of cycling deoxygenation. These data suggest that ET-1-mediated reduction in Mg^{2+} efflux might be mediated by NME activity. The data further support the idea that erythrocyte dehydration during cycling deoxygenation engages not only K^+ efflux transporters but also Mg^{2+} efflux contributing to sickle red cell dehydration.

3.3 | ET-1 blocks deoxygenation-stimulated dehydration of human red cells in the presence of Gardos channel blocker

Erythrocytes dehydrate during periods of deoxygenation through activation of K^+ efflux through K^+ transporters such as KCC K-Cl cotransporters or the KCNN4/KCa3.1 Gardos channel.[51–53] We tested the effect of ET-1-induced dehydration in the absence of the Gardos channel activity. Cycling deoxygenation for 3 h produced a significantly greater rightward shift in the density profile of SCD (SS) erythrocytes (Figure 4B) than in normal (AA) red cells (Figure 4A). A subpopulation of normal AA red cells responded to cycling deoxygenation with greater dehydration (Figure 4A). In normal erythrocytes, ET-1 significantly reduced dehydration in this subpopulation, but the effect of ET-1 on SCD cell density was greatly attenuated. The presence of 100 μM imipramine in combination with ET-1 significantly reversed ET-1-induced dehydration in both sickle and normal erythrocytes. However, although the ETRB antagonist blocked erythrocyte dehydration in sickle erythrocytes, this was not the case in normal AA red cells. Cycling deoxygenation induced significant cell dehydration in SCD SS erythrocytes even in the presence of 10 μM Gardos channel inhibitor, clotrimazole, but failed to significantly dehydrate normal AA red cells. The

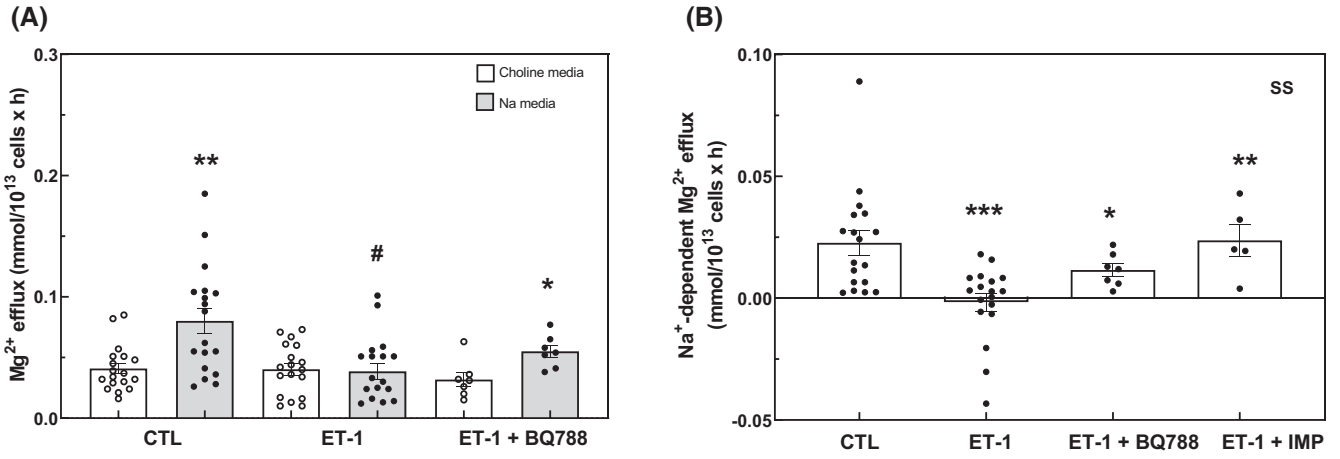

FIGURE 3 Cyclic deoxygenation decreases ET-1-stimulated Mg^{2+} transport sensitive to BQ788 and to imipramine in ex vivo human sickle erythrocytes. Sickle red cell suspensions were exposed to cyclic deoxygenation for 3 h. Mg^{2+} efflux was then measured in Mg^{2+}-unloaded red cells. ET-1, 500 nM; BQ788, 1 μM; Imipramine (IMP), 100 μM. (A) Mg^{2+} efflux in the absence or presence of extracellular Na^+. $^*p = .015$, $^{**}p = .0001$ vs. CTL in each condition; $^{\#}p = .0003$ compared with CTL in Na media; Wilcoxon test for matched data. (B) Na^+-dependent Mg^{2+} efflux. Data are means ± SEM from ≥7 independent triplicate experiments. $^*p = .021$ for ET-1 vs. ET-1 + BQ788; $^{**}p = .0025$ for ET-1 vs. ET-1 + IMP; $^{***}p = .0005$ for ET-1 vs. CTL. Mann–Whitney test for unpaired data. CTL vs. ET-1 + BQ788 and CTL vs. IMP comparisons were not statistically significant.

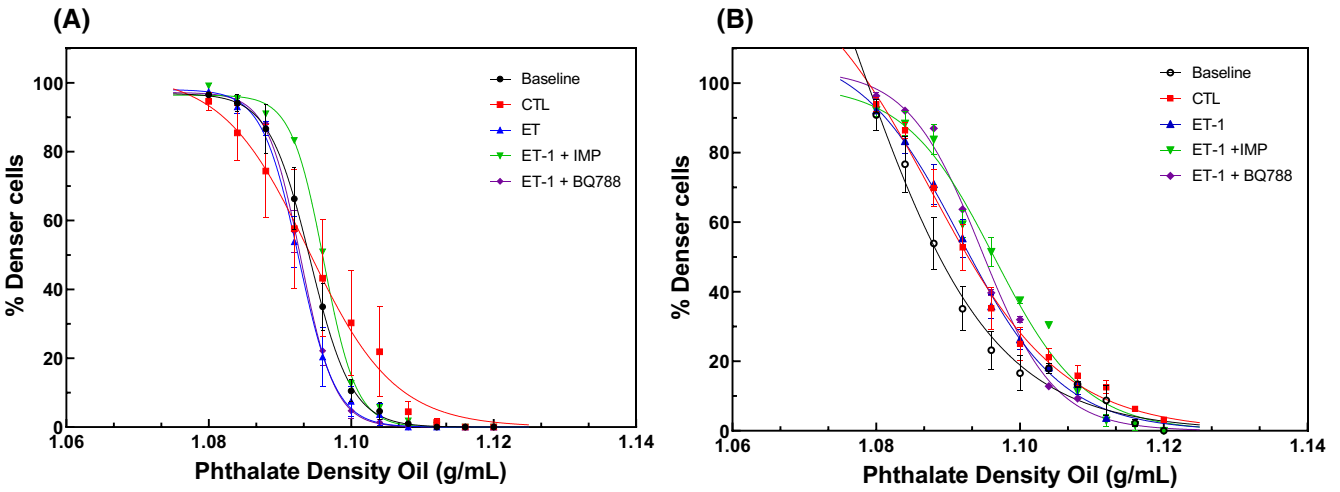

FIGURE 4 Red cell density distribution in normal (A) and in sickle erythrocytes (B). Density distribution profiles were measured at baseline (black, in-room air) and subsequently after 3 h cyclic deoxygenation in the absence (red squares), CTL) or presence of 500 nM ET-1 (blue triangles), 100 μM Imipramine (green inverted triangles, IMP) or 1 μM BQ788 (purple diamonds) (see *Methods*). Data are means ± SEM of 5 triplicate experiments. D_{50} values (see Table 1) were calculated from curves fit to sigmoid equations (GraphPad PRISM 9.0).

presence of 500 nM ET-1 during cycling deoxygenation significantly shifted the D_{50} in a manner blocked by the presence of imipramine or of BQ788, suggesting possible mediation of this effect by Mg^{2+} efflux via NME.

3.4 | Na^+/Mg^{2+} exchange is enhanced in a mouse model of sickle cell disease

We examined NME activity in various well-studied mouse models of SCD. Heparinized whole blood was collected and processed as described in Methods. Figure 5 shows that maximal NME activity in Mg^{2+}-loaded red cells was significantly higher in red cells from each studied mouse SCD model than in red cells of wild-type (WT) mice. In contrast, rates of Na^+-independent Mg^{2+} efflux were greatly reduced only in red cells from the SAD mouse model of SCD. However, only red cells from BERK and NY1DD mice exhibited significantly higher Mg^{2+} content than WT red cells, despite their elevated rates of NME and (in BERK only) Na^+-independent Mg^{2+} efflux.

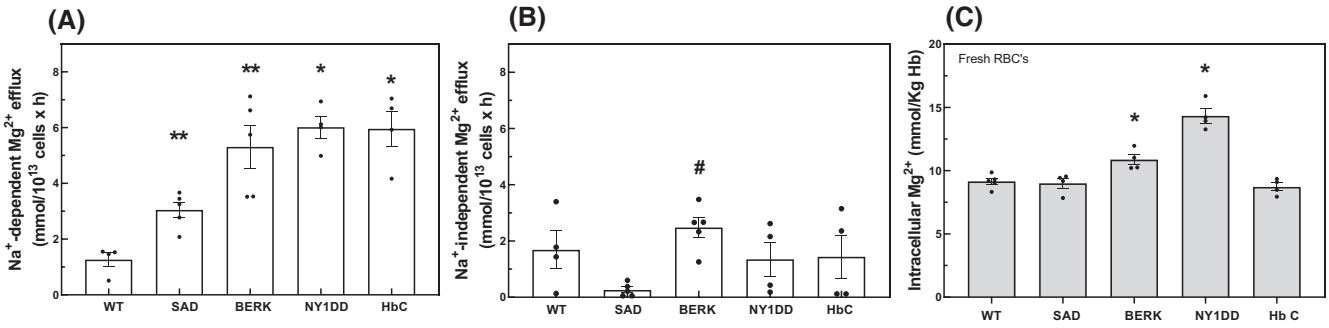

FIGURE 5 Na^+/Mg^{2+} exchange activity in red cells from several mouse models of hemoglobinopathies. (A) Na^+-dependent Mg^{2+} efflux was measured in red cells of mouse hemoglobinopathy models as described in *Methods*. These included Wild-type mice (WT: C57Bl/6j), SAD,[45] BERK[42] and NY1DD[44] mouse models of sickle cell disease, and human HbC-expressing mice.[43] Values represent means ± SEM for ≥3 quadruplicate experiments. *$p = .02$; **,$p = .015$ vs. WT. (B) Na^+-independent Mg^{2+} efflux was measured in Choline Cl media. Values represent means ± SEM of ≥3 quadruplicate experiments. #$p = .008$ BERK vs. SAD. (C) Post-loading Mg^{2+} content in red cells from the indicated mouse hemoglobinopathy models. Values represent means ± SEM of 3 quadruplicate experiments. *$p = .039$ vs. WT. Mann–Whitney test.

3.5 | ET-1 plasma levels are elevated in red cells from mouse models of SCD

ET-1 plasma levels have been reported elevated in sickle cell patients during and after acute painful crises.[10,54,55] SCD patients at steady state have elevated plasma cytokines such as PGE2 and ET-1, as compared with control subjects. These elevated cytokine levels are believed to contribute to the vascular pathology of SCD. ET-1 has been postulated to play an important role in initiation of the painful crises of SCD.[10,56] To evaluate a possible relationship between elevated NME and elevated plasma ET-1 levels, we collected plasma and measured ET-1 levels as described in Methods. We found red cells of all transgenic mouse models of SCD tested exhibited elevated plasma levels of ET-1 (Table 2). This relationship suggests that elevated steady state inflammation in mouse models of SCD could contribute to the detected elevated rates of NME-mediated Mg^{2+} efflux.

3.6 | In vivo treatment with endothelin-1 receptor antagonist reduces Na^+/Mg^{2+} exchange in BERK mice

We have previously reported that the elevated K^+ transport mediated by the erythroid Gardos channel KCNN4 in SAD mouse red cells was significantly reduced by in vivo treatment with a mixture of ETRA and ETRB antagonists.[11,57] This reduction of Gardos channel activity was accompanied by improved erythrocyte dehydration status, along with several additional changes in hematological parameters. These observations suggested that reduction of the elevated circulating ET-1 levels in SCD might be of clinical benefit. We, therefore, investigated the effect of ETR antagonists on NME in vitro and in vivo. Figure 6A presents the effects of ET-1 on NME activity in the presence or absence of ETRB antagonist (BQ788) in BERK mice. We observed that NME activity was significantly elevated by ET-1 and blunted by the additional presence of BQ788, suggesting that NME is regulated by ET-1 via ETRB. A 14-day treatment of BERK mice with a mixture of selective ETRA (BQ123) and ETRB (BQ788) showed significant reductions in both total Mg^{2+} efflux and NME. Together, these results support the hypothesis that ET-1 receptor antagonists can modulate sickle red cell dehydration status by regulating Mg^{2+} homeostasis.

3.7 | Effects of inflammatory cytokine on Na^+/Mg^{2+} exchange activity

We previously observed that the physiological regulation of NME by intracellular signaling pathways such as PKC and phosphatases was altered in sickle erythrocytes in a manner suggesting constitutive activation of NME.[41] We were therefore prompted to investigate whether circulating cytokines known to be pathologically elevated in SCD[10,58–60] also might regulate NME. We measured NME activity in the absence or presence of 100 nM PAF, 100 nM PGE2, or 40 ng/ml RANTES in human normal (AA) and sickle (SS) erythrocytes (Figure 7). We observed that all three cytokines significantly increased NME activity in both cell types (Figure 7A). In contrast, Na^+-independent Mg^{2+} efflux from SS red cells was unaffected by PAF, PGE2 or RANTES. However, Na^+-independent Mg^{2+} efflux in the presence of PGE2 was significantly lower in SS vs. AA red cells. Similar trends were observed in the presence of PAF or RANTES but did not reach significance (Figure 7B). These results together suggest that red cell

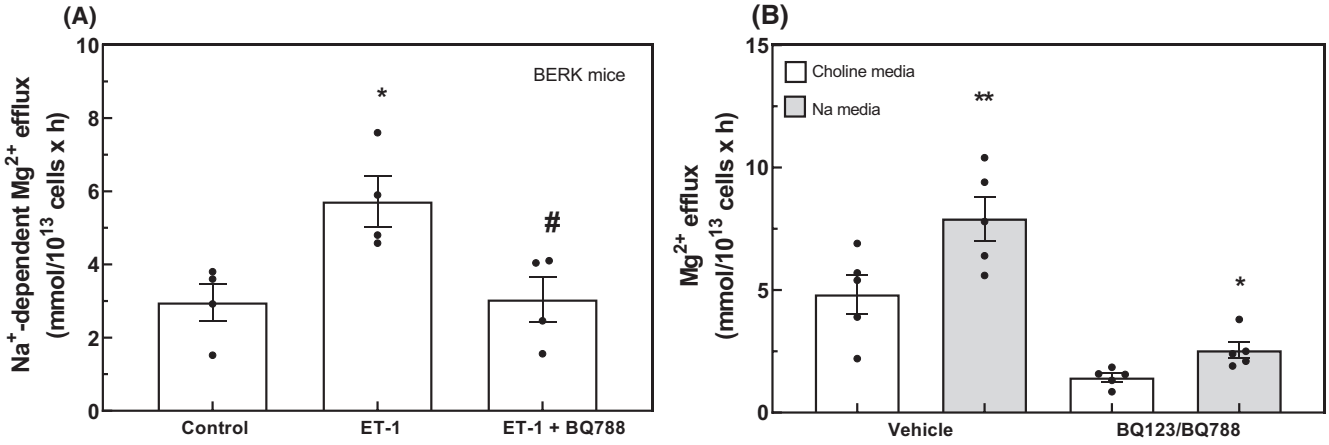

FIGURE 6 The selective ETB receptor antagonist, BQ788, inhibits ET-1-stimulated NME activity in sickle mouse erythrocytes. (A) In vitro Na^+-dependent Mg^{2+} efflux was measured in Mg-loaded red cells from BERK mice, in the presence or absence of 500 nM ET-1 and 1 μM BQ788. Bars represent means ± S.E.M of ≥3 triplicate experiments. *$p < .028$ for Control vs. ET-1); #$p < .03$ for ET-1 vs. ET_1 + BQ788. Mann–Whitney test. ET-1 + BQ788 did not differ from Control. (B) BERK mice of ~4 months of age were injected i.p. for 14 days with an ETR antagonists cocktail containing a 1:1 mix of an ETRB antagonist BQ788 and ETRA antagonist BQ123, as described in Methods. Mg^{2+} efflux was measured in the extracellular presence of choline (white bars) or Na^+ (gray bars). *$p = .035$; **$p = .0003$ vs. choline Cl media, by Wilcoxon rank test.

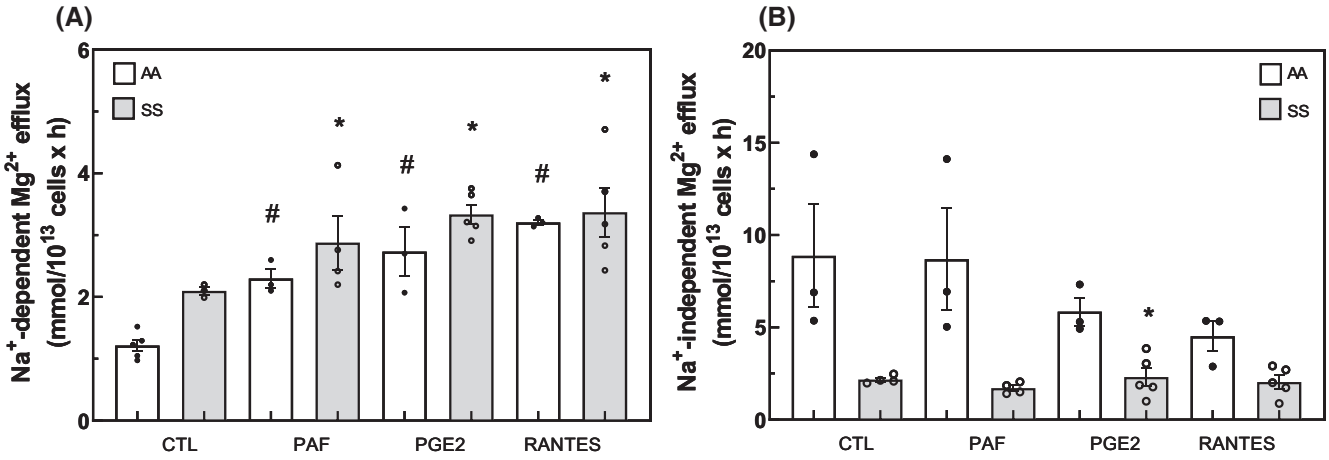

FIGURE 7 Cytokine regulation of NME in human AA and SS erythrocytes. Mg^{2+}-loaded AA (white bars) and SS red cells (gray bars) were subjected to measurement of NME at 37°C in the absence or presence of 100 nM platelet-activating factor (PAF), 100 nM prostaglandin E2 (PGE2) or 40 ng/ml RANTES. (A) Na^+-dependent Mg^{2+} efflux. #$p < .04$ (CTL vs. each cytokine) in AA cells; *$p < .04$ (control vs. each cytokine in SS cells). (B) Na^+-independent Mg^{2+} efflux. *$p = .0357$ (SS + PGE2 vs. AA + PGE2). Means ± SEM of >3 triplicate determinations. Mann–Whitney test. Differences between CTL and each cytokine did not achieve significance in AA or SS red cells.

Mg^{2+} homeostasis is regulated by the elevated cytokine levels characteristic of SCD.

4 | DISCUSSION

Erythrocytes have very low permeability for Mg^{2+} under normal conditions.[36,61,62] Mg^{2+} inside red cells is far from electrochemical equilibrium, suggesting the presence of an active Mg^{2+} extrusion pathway. Hemoglobin S polymerization has been proposed to promote Mg^{2+} loss in sickle erythrocytes.[27] We and others have documented elevated NME activity in human sickle erythrocytes as compared to normal red cells.[29,40,41] We now report that ET-1 regulates NME activity and cellular hydration status in human and mouse sickle erythrocytes (Figures 1, 2, and 5).

Cytokines play an important role in the adhesion of sickle erythrocytes to the endothelium and the pathogenesis of vaso-occlusive episodes of SCD.[5,6,10] However, the physiological roles of cytokines and chemokine receptors in erythrocytes remain unclear, but clearance of free chemokines from circulation has been proposed as

ID	AA D_{50}, g/ml	SS
Baseline	1.094 ± 0.0001 ($n = 6$)	1.076 ± 0.0009 ($n = 4$)
Control	1.094 ± 0.003 ($n = 6$)	1.088 ± 0.003 ($n = 6$)**
500 nM ET-1	1.093 ± 0.0001 ($n = 6$)	1.092 ± 0.001 ($n = 5$)***
500 nM ET-1 + 100 μM Imipramine	1.096 ± 0.0001 ($n = 5$)	1.096 ± 0.0006 ($n = 3$)*
500 nM ET-1 + 1 μM BQ788	1.092 ± 0.001 ($n = 5$)	1.095 ± 0.0003 ($n = 3$)*

TABLE 1 Density at 50% (D_{50}) in SS vs. AA erythrocytes after 3 h of deoxy/oxygenation cycles at 37°C in normal saline in the presence or absence of 500 nM ET-1 with or without 1 μM BQ788 or 100 μM imipramine

Note: Density at 50% (D_{50}) was estimated from the sigmoidal curve of the density profile in panel A and B using GraphPad software. ET-1, endothelin-1; BQ788, selective inhibitor of endothelin-1 receptor B subtype. Values represent mean ± SEM of n determinations, *$p = .025$, **$p = .004$, ***$p = .001$. Mann–Whitney test, nonparametric. No significant differences among AA values.

TABLE 2 Endothelin-1 plasma levels in different hemoglobin in mouse erythrocytes compared to Wild Type

ID	ET-1, pmol/ml
C57bl/6j	122.2 ± 25 ($n = 3$)
CD-1	148.3 ± 18 ($n = 4$)
SAD	220.1 ± 31 ($n = 3$)*
BERK	321.2 ± 30 ($n = 3$)***
NY1DD	298.5 ± 15 ($n = 3$)**

Note: ET-1 concentration were determined by HPLC. Values represent mean ± SEM. *$p = .02$, **$p = .01$, ***$p = .001$ (Mann–Whitney test, nonparametric) vs. C57bl/6j mice.

a function.[63] Activation of receptors for cytokines and chemokines leads to a sustained increase in intracellular Ca^{2+} in various cell types,[64–66] suggesting a mechanism for activation of the erythroid Gardos channel.[48] The erythroid chemokine receptor is identical to the Duffy antigen, which also functions as a receptor for *Plasmodium vivax*.[67] We previously reported that the Duffy antigen/chemokine receptor might also regulate erythrocyte volume, as we found that RANTES and PAF significantly modulated Gardos channel activity.[48] In addition, the absence of Gardos channel stimulation by RANTES in Duffy-negative erythrocytes suggested a potentially specific interaction of the receptor with the Gardos channel.[48] Here, we observed that the chemokine receptor ligand, RANTES, can also modulate NME (Figure 7). Gardos channel activators PAF and PGE2 also increased NME activity, suggesting an interplay among these red cell volume regulatory systems to control erythrocyte hydration. ET-1 receptor activation may induce a signaling cascade including intracellular Ca^{2+} elevation and Mg^{2+} efflux to promote dehydration and endothelial cell adhesion, both in turn increasing susceptibility to hypoxic sickling and to vaso-occlusive crisis.

Previous studies have proposed that sickle erythrocytes but not normal red cells exhibit increased Mg^{2+} permeabilization during deoxygenation.[27] Ortiz et al showed that, in the presence of EDTA, sickle red cell Mg content was decreased in both discocytes and the densest fraction of sickle erythrocytes subjected to 2 h of deoxygenation. In the current study, we report that Mg^{2+} flux was stimulated by deoxygenation in sickle erythrocytes (Figure 3A) and was very sensitive to the presence of extracellular Na^+, strongly suggesting that Mg^{2+} transport under low oxygen tension was mediated by a Na^+-dependent mechanism. We observed that ET-1 preincubation led to the reduction of NME. These results suggest that ET-1 modifies deoxygenation-regulated Mg^{2+} fluxes (Figure 3B). Further characterization of this pathway indicated that ET-1's effect on NME was mediated by ETRB (Figure 3A,B). In addition, ET-1-induced deoxygenation-regulated Mg^{2+} efflux was blocked by imipramine, an inhibitor of NME.

These results support the idea that Mg^{2+} plays an important role in sickle erythrocyte hydration status in vivo. In fact, ET-1–mediated dehydration during repeated cyclic deoxygenation of sickle but not of normal erythrocytes was reduced in the presence of imipramine (Figure 4A,B). Imipramine right-shifted the sickle red cell density profile, with a significant change in D_{50}, suggesting that sickle red cell dehydration by ET-1 in the absence of Gardos channel activity was influenced by Mg^{2+} flux. This response suggests an active role for the Mg^{2+}-regulated fraction of red cell K-Cl cotransport activity. We further observed that ET-1 antagonists were effective in blocking ET-1-stimulated sickle erythrocyte dehydration (Table 1). These data suggest that, during cyclic deoxygenation, the Gardos channel[48] and K-Cl cotransport both contribute to red cell volume regulation. Therefore, in vivo pharmacological blockade of NME might be beneficial in maintaining sickle erythrocyte hydration status.

To investigate the possible presence of elevated NME in erythrocytes from mouse models of SCD, we measured NME in several well-established mouse models. We found that mouse sickle erythrocytes also exhibited significantly elevated NME as compared to red cells from WT mice (Figure 5). We also observed that Na^+-independent Mg^{2+} efflux from red cells was significantly higher in cells from BERK mice than in those of SAD

mice, but elevated Na^+-independent Mg^{2+} efflux was not observed in red cells from NY1DD or Hb C mice. These Mg^{2+} efflux activities were accompanied by higher Mg^{2+} content in BERK and NY1DD sickle erythrocytes than in red cells from WT mice. In contrast, Mg^{2+} content of human sickle erythrocytes (1.97 ± 0.049 mmol/L cells, $n = 18$) was lower than in normal human red cells (2.37 ± 0.08 mmol/L cells, $n = 82$; $p = .004$). The mechanism(s) underlying this difference is/are unknown. Feillet-Coudray et al. proposed that genetic regulation of mouse red cell Mg^{2+} content[68] can be modulated by nutritional status,[69] consistent with multifactorial regulation of Mg^{2+} homeostasis in mouse red cells, perhaps mediated by Mg^{2+} transporters such as TRPM channels,[70] SLC41A1[71] and/or H^+/Mg^{2+} exchange.[72] However, the proposed function of human SLC41A1 as a Na^+/Mg^{2+} exchanger[35,73] has been countered by the recent demonstration that SLC41A1-mediated Mg^{2+} transport is Na^+-independent.[34] Further studies are thus needed to assess and define the Mg^{2+} transport systems contributing to Mg^{2+} homeostasis in mouse red cells.

The interaction of sickle erythrocytes with vascular endothelial cells stimulates the release of ET-1 and regulates ET-1 gene expression in cultured endothelial cells.[74] However, the ability of increased plasma levels of ET-1 to modulate red cell Mg^{2+} transport in vivo has remained unknown. We have shown that mouse models of SCD share the human SCD phenotype of elevated plasma levels of ET-1.[10] Table 2 confirms that plasma ET-1 levels in SAD, BERK, and NY1DD transgenic mice were higher than those in WT mice. These results suggest that the increased circulating cytokine levels in mouse models of SCD might also contribute to the elevated NME of mouse sickle erythrocytes.

Although the ET-1 concentration required to stimulate red cell Mg^{2+} transport in vitro exceeds levels documented in plasma from patients during a painful crisis, it is likely that local levels of ET-1 greatly exceed those measured systemically. We have shown that in BERK mouse red cells, ET-1 stimulation of increased NME is blocked by the ETRB inhibitor, BQ788 (Table 2). We, therefore, investigated if in vivo treatment of BERK mice with ET1 receptor antagonists would affect NME in red cells. We observed that combined treatment with ETRA and ETRB antagonists effectively inhibited NME in red cells, suggesting their potential use as an adjuvant treatment of human SCD to reduce red cell dehydration in vivo. However, we also observed significant inhibition by the ET-1 antagonists of Na^+-independent Mg^{2+} efflux, suggesting the likely importance of both Na^+-dependent and -independent Mg^{2+} efflux pathways in regulating red cell dehydration status. Further characterization of both red cell pathways will be required to understand their roles more clearly in human SCD pathophysiology, as well as in other disorders of cellular and tissue Mg^{2+} homeostasis.

AUTHOR CONTRIBUTIONS

A preliminary report of these findings was presented in abstract form. The study was conceived and designed by Alicia Rivera and José R. Romero. Collection and/or assembly of data was done by Patricia Pulido-Perez, Pablo Lopez, José R. Romero, and Alicia Rivera. Data analyses and interpretation were done by José R. Romero, Yaritza Inostroza-Nieves, and Alicia Rivera. The manuscript was written by José R. Romero, Seth L. Alper, and Alicia Rivera, and revised by José R. Romero, Jay G. Wohlgemuth, Jeffrey S. Dlott, L. Michael Snyder, Seth L. Alper, and Alicia Rivera.

ACKNOWLEDGMENTS

We thank Dr. Mary E. Fabry and Mrs. Sandra Suzuka for their kind support and advice during the development of the sickle mouse colony. We thank Dr. Carlo Brugnara for support and critical input. We also express our gratitude to the students in our *Translational Research Summer Program for Medical Students* at the Brigham and Women's Hospital / Harvard Medical School. This work was supported by NIH grants HL67699 and HL090632 to AR, and DK06484 and HL096518 to JRR.

DISCLOSURES

JGW and JSD are employees and stockholders of Quest Diagnostics Inc. SLA and LMS are consultants to Quest Diagnostics Inc. SLA received research support from Quest Diagnostics Inc.

DATA AVAILABILITY STATEMENT

The data that support the findings of this study are available in the methods and/or supplementary material of this article.

ORCID

Seth L. Alper https://orcid.org/0000-0002-6228-2512
Alicia Rivera https://orcid.org/0000-0002-0433-6367

REFERENCES

1. Platt OS, Thorington BD, Brambilla DJ, et al. Pain in sickle cell disease. Rates and risk factors. *N Engl J Med*. 1991;325(1):11-16.
2. Platt OS, Brambilla DJ, Rosse WF, et al. Mortality in sickle cell disease. Life expectancy and risk factors for early death. *N Engl J Med*. 1994;330(23):1639-1644.
3. Steinberg MH. Management of sickle cell disease. *N Engl J Med*. 1999;340(13):1021-1030.
4. Musa BO, Onyemelukwe GC, Hambolu JO, Mamman AI, Isa AH. Pattern of serum cytokine expression and T-cell subsets in sickle cell disease patients in vaso-occlusive crisis. *Clin Vaccine Immunol*. 2010;17(4):602-608.

5. Croizat H, Nagel RL. Circulating cytokines response and the level of erythropoiesis in sickle cell anemia. *Am J Hematol*. 1999;60(2):105-115.
6. Bourantas KL, Dalekos GN, Makis A, Chaidos A, Tsiara S, Mavridis A. Acute phase proteins and interleukins in steady state sickle cell disease. *Eur J Haematol*. 1998;61(1):49-54.
7. Khodorova A, Navarro B, Jouaville LS, et al. Endothelin-B receptor activation triggers an endogenous analgesic cascade at sites of peripheral injury. *Nat Med*. 2003;9(8):1055-1061.
8. Kaul DK, Liu XD, Zhang X, Ma L, Hsia CJ, Nagel RL. Inhibition of sickle red cell adhesion and vasoocclusion in the microcirculation by antioxidants. *Am J Physiol Heart Circ Physiol*. 2006;291(1):H167-H175.
9. Rybicki AC, Benjamin LJ. Increased levels of endothelin-1 in plasma of sickle cell anemia patients. *Blood*. 1998;92(7):2594-2596.
10. Graido-Gonzalez E, Doherty JC, Bergreen EW, Organ G, Telfer M, McMillen MA. Plasma endothelin-1, cytokine, and prostaglandin E2 levels in sickle cell disease and acute vaso-occlusive sickle crisis. *Blood*. 1998;92(7):2551-2555.
11. Rivera A. Reduced sickle erythrocyte dehydration in vivo by endothelin-1 receptor antagonists. *Am J Physiol Cell Physiol*. 2007;293(3):C960-C966.
12. Ferreira A, Rivera A, Romero JR. Na^+/Mg^{2+} exchange is functionally coupled to the insulin receptor. *J Cell Physiol*. 2004;199(3):434-440.
13. Ferreira A, Rivera A, Wohlgemuth JG, et al. Dysregulated erythroid Mg(2+) efflux in type 2 diabetes. *Front Cell Dev Biol*. 2022;10:861644.
14. Nielsen FH. Magnesium deficiency and increased inflammation: current perspectives. *J Inflamm Res*. 2018;11:25-34.
15. Moslehi N, Vafa M, Rahimi-Foroushani A, Golestan B. Effects of oral magnesium supplementation on inflammatory markers in middle-aged overweight women. *J Res Med Sci*. 2012;17(7):607-614.
16. Maier JA, Castiglioni S, Locatelli L, Zocchi M, Mazur A. Magnesium and inflammation: Advances and perspectives. *Semin Cell Dev Biol*. 2021;115:37-44.
17. Altura RA, Wang WC, Wynn L, Altura BM, Altura BT. Hydroxyurea therapy associated with declining serum levels of magnesium in children with sickle cell anemia. *J Pediatr*. 2002;140(5):565-569.
18. Yousif OO, Hassan MK, Al-Naama LM. Red blood cell and serum magnesium levels among children and adolescents with sickle cell anemia. *Biol Trace Elem Res*. 2018;186(2):295-304.
19. Gao F, Ding B, Zhou L, Gao X, Guo H, Xu H. Magnesium sulfate provides neuroprotection in lipopolysaccharide-activated primary microglia by inhibiting NF-kappaB pathway. *J Surg Res*. 2013;184(2):944-950.
20. Ferre S, Baldoli E, Leidi M, Maier JA. Magnesium deficiency promotes a pro-atherogenic phenotype in cultured human endothelial cells via activation of NFkB. *Biochim Biophys Acta*. 2010;1802(11):952-958.
21. Jimenez JS, Benitez MJ, Lechuga CG, Collado M, Gonzalez-Nicolas J, Moreno FJ. Casein kinase 2 inactivation by Mg^{2+}, Mn^{2+} and Co^{2+} ions. *Mol Cell Biochem*. 1995;152(1):1-6.
22. Ebel H, Kreis R, Gunther T. Regulation of Na^+/Mg^{2+} antiport in rat erythrocytes. *Biochim Biophys Acta*. 2004;1664(2):150-160.
23. Altura BM, Shah NC, Shah GJ, et al. Short-term Mg deficiency upregulates protein kinase C isoforms in cardiovascular tissues and cells; relation to NF-kB, cytokines, ceramide salvage sphingolipid pathway and PKC-zeta: hypothesis and review. *Int J Clin Exp Med*. 2014;7(1):1-21.
24. Libien J, Sacktor TC, Kass IS. Magnesium blocks the loss of protein kinase C, leads to a transient translocation of PKC(alpha) and PKC(epsilon), and improves recovery after anoxia in rat hippocampal slices. *Brain Res Mol Brain Res*. 2005;136(1–2):104-111.
25. Pedrosa AM, Lemes RPG. Gene expression of HIF-1alpha and VEGF in response to hypoxia in sickle cell anaemia: Influence of hydroxycarbamide. *Br J Haematol*. 2020;190(1):e39-e42.
26. Lehmann H. Treatment of sickle-cell anemia. *Br Med J*. 1963;1(5338):1158-1159.
27. Ortiz OE, Lew VL, Bookchin RM. Deoxygenation permeabilizes sickle cell anaemia red cells to magnesium and reverses its gradient in the dense cells. *J Physiol*. 1990;427:211-226.
28. Brugnara C, De Franceschi L, Armsby CC, et al. A new therapeutic approach for sickle cell disease. Blockade of the red cell Ca(2+)-activated K^+ channel by clotrimazole. *Ann N Y Acad Sci*. 1995;763:262-271.
29. De Franceschi L, Bachir D, Galacteros F, et al. Oral magnesium pidolate: effects of long-term administration in patients with sickle cell disease. *Br J Haematol*. 2000;108(2):284-289.
30. De Franceschi L, Beuzard Y, Jouault H, Brugnara C. Modulation of erythrocyte potassium chloride cotransport, potassium content, and density by dietary magnesium intake in transgenic SAD mouse. *Blood*. 1996;88(7):2738-2744.
31. Hankins JS, Wynn LW, Brugnara C, Hillery CA, Li CS, Wang WC. Phase I study of magnesium pidolate in combination with hydroxycarbamide for children with sickle cell anaemia. *Br J Haematol*. 2008;140(1):80-85.
32. Schlingmann KP, Gudermann T. A critical role of TRPM channel-kinase for human magnesium transport. *J Physiol*. 2005;566(Pt 2):301-308.
33. Kolisek M, Launay P, Beck A, et al. SLC41A1 is a novel mammalian Mg^{2+} carrier. *J Biol Chem*. 2008;283(23):16235-16247.
34. Arjona FJ, Latta F, Mohammed SG, et al. SLC41A1 is essential for magnesium homeostasis in vivo. *Pflugers Arch*. 2019;471(6):845-860.
35. Kolisek M, Nestler A, Vormann J, Schweigel-Rontgen M. Human gene SLC41A1 encodes for the Na^+/Mg^{2+} exchanger. *Am J Physiol Cell Physiol*. 2012;302(1):C318-C326.
36. Feray JC, Garay R. An Na^+-stimulated Mg^{2+}-transport system in human red blood cells. *Biochim Biophys Acta*. 1986;856(1):76-84.
37. Gunther T. Mechanisms and regulation of Mg^{2+} efflux and Mg^{2+} influx. *Miner Electrolyte Metab*. 1993;19(4–5):259-265.
38. Xu W, Willis JS. Sodium transport through the amiloride-sensitive Na-Mg pathway of hamster red cells. *J Membr Biol*. 1994;141(3):277-287.
39. Touyz RM, Yao G. Inhibitors of Na^+/Mg^{2+} exchange activity attenuate the development of hypertension in angiotensin II-induced hypertensive rats. *J Hypertens*. 2003;21(2):337-344.
40. Feray JC, Garay R. Demonstration of a Na^+: Mg^{2+} exchange in human red cells by its sensitivity to tricyclic antidepressant drugs. *Naunyn Schmiedebergs Arch Pharmacol*. 1988;338(3):332-337.
41. Rivera A, Ferreira A, Bertoni D, Romero JR, Brugnara C. Abnormal regulation of Mg^{2+} transport via Na/Mg exchanger in sickle erythrocytes. *Blood*. 2005;105(1):382-386.

42. Paszty C, Brion CM, Manci E, et al. Transgenic knockout mice with exclusively human sickle hemoglobin and sickle cell disease. *Science*. 1997;278(5339):876-878.
43. Romero JR, Suzuka SM, Nagel RL, Fabry ME. Expression of HbC and HbS, but not HbA, results in activation of K-Cl cotransport activity in transgenic mouse red cells. *Blood*. 2004;103(6):2384-2390.
44. Ginzburg YZ, Andorfer JH, Rybicki AC, Fabry ME, Nagel RL. Murine glutathione S-transferase A1-1 in sickle transgenic mice. *Am J Hematol*. 2007;82(10):911-915.
45. Trudel M, Saadane N, Garel MC, et al. Towards a transgenic mouse model of sickle cell disease: hemoglobin SAD. *EMBO J*. 1991;10(11):3157-3165.
46. Kurantsin-Mills J, Jacobs HM, Lessin LS. Assessment of the hydration state of sickle cells by phthalate ester density distribution. *J Lab Clin Med*. 1987;109(4):486-494.
47. Bartolucci P, Brugnara C, Teixeira-Pinto A, et al. Erythrocyte density in sickle cell syndromes is associated with specific clinical manifestations and hemolysis. *Blood*. 2012;120(15):3136-3141.
48. Rivera A, Jarolim P, Brugnara C. Modulation of Gardos channel activity by cytokines in sickle erythrocytes. *Blood*. 2002;99(1):357-603.
49. Ferri C, Bellini C, Desideri G, Mazzocchi C, De Siati L, Santucci A. Elevated plasma and urinary endothelin-I levels in human salt-sensitive hypertension. *Clin Sci (Lond)*. 1997;93(1):35-41.
50. Ebel H, Hollstein M, Gunther T. Differential effect of imipramine and related compounds on Mg^{2+} efflux from rat erythrocytes. *Biochim Biophys Acta*. 2004;1667(2):132-140.
51. Geisness AC, Azul M, Williams D, et al. Ionophore-mediated swelling of erythrocytes as a therapeutic mechanism in sickle cell disease. *Haematologica*. 2022;107(6):1438-1447.
52. Rab MAE, van Oirschot BA, Bos J, et al. Characterization of sickling during controlled automated deoxygenation with oxygen gradient ektacytometry. *J Vis Exp*. 2019;153:1-10.
53. Shmukler BE, Rivera A, Bhargava P, et al. Combined genetic disruption of K-Cl cotransporters and Gardos channel KCNN4 rescues erythrocyte dehydration in the SAD mouse model of sickle cell disease. *Blood Cells Mol Dis*. 2019;79:102346.
54. Ergul S, Brunson CY, Hutchinson J, et al. Vasoactive factors in sickle cell disease: in vitro evidence for endothelin-1-mediated vasoconstriction. *Am J Hematol*. 2004;76(3):245-251.
55. Kalish BT, Matte A, Andolfo I, et al. Dietary omega-3 fatty acids protect against vasculopathy in a transgenic mouse model of sickle cell disease. *Haematologica*. 2015;100(7):870-880.
56. Angerio AD, Lee ND. Sickle cell crisis and endothelin antagonists. *Crit Care Nurs Q*. 2003;26(3):225-229.
57. Prado GN, Romero JR, Rivera A. Endothelin-1 receptor antagonists regulate cell surface-associated protein disulfide isomerase in sickle cell disease. *FASEB J*. 2013;27(11):4619-4629.
58. Oh SO, Ibe BO, Johnson C, Kurantsin-Mills J, Raj JU. Platelet-activating factor in plasma of patients with sickle cell disease in steady state. *J Lab Clin Med*. 1997;130(2):191-196.
59. Chadebech P, de Menorval MA, Bodivit G, et al. Cytokine changes in sickle-cell disease patients as markers predictive of the onset of delayed hemolytic transfusion reactions. *Cytokine*. 2020;136:155259.
60. Durpes MC, Nebor D, du Mesnil PC, et al. Effect of interleukin-8 and RANTES on the Gardos channel activity in sickle human red blood cells: role of the Duffy antigen receptor for chemokines. *Blood Cells Mol Dis*. 2010;44(4):219-223.
61. Gunther T, Vormann J. Mg^{2+} efflux is accomplished by an amiloride-sensitive Na^+/Mg^{2+} antiport. *Biochem Biophys Res Commun*. 1985;130(2):540-545.
62. Ludi H, Schatzmann HJ. Some properties of a system for sodium-dependent outward movement of magnesium from metabolizing human red blood cells. *J Physiol*. 1987;390:367-382.
63. Szabo MC, Soo KS, Zlotnik A, Schall TJ. Chemokine class differences in binding to the Duffy antigen-erythrocyte chemokine receptor. *J Biol Chem*. 1995;270(43):25348-25351.
64. Salter KJ, Turner JL, Albarwani S, Clapp LH, Kozlowski RZ. Ca(2+)-activated Cl^- and K^+ channels and their modulation by endothelin-1 in rat pulmonary arterial smooth muscle cells. *Exp Physiol*. 1995;80(5):815-824.
65. Brailoiu E, Barlow CL, Ramirez SH, Abood ME, Brailoiu GC. Effects of platelet-activating factor on brain microvascular endothelial cells. *Neuroscience*. 2018;377:105-113.
66. Ahmed S, Kim Y. PGE2 mediates hemocyte-spreading behavior by activating aquaporin via cAMP and rearranging actin cytoskeleton via Ca(2). *Dev Comp Immunol*. 2021;125:104230.
67. Miller LH, Mason SJ, Dvorak JA, McGinniss MH, Rothman IK. Erythrocyte receptors for (Plasmodium knowlesi) malaria: Duffy blood group determinants. *Science*. 1975;189(4202):561-563.
68. Feillet-Coudray C, Coudray C, Wolf FI, Henrotte JG, Rayssiguier Y, Mazur A. Magnesium metabolism in mice selected for high and low erythrocyte magnesium levels. *Metabolism*. 2004;53(5):660-665.
69. Feillet-Coudray C, Trzeciakiewicz A, Coudray C, et al. Erythrocyte magnesium fluxes in mice with nutritionally and genetically low magnesium status. *Eur J Nutr*. 2006;45(3):171-177.
70. Schlingmann KP, Weber S, Peters M, et al. Hypomagnesemia with secondary hypocalcemia is caused by mutations in TRPM6, a new member of the TRPM gene family. *Nat Genet*. 2002;31(2):166-170.
71. Sponder G, Rutschmann K, Kolisek M. "Inside-in" or "inside-out"? The membrane topology of SLC41A1. *Magnes Res*. 2013;26(4):176-181.
72. Aromataris EC, Roberts ML, Barritt GJ, Rychkov GY. Glucagon activates Ca^{2+} and Cl^- channels in rat hepatocytes. *J Physiol*. 2006;573(Pt 3):611-625.
73. Sahni J, Nelson B, Scharenberg AM. SLC41A2 encodes a plasma-membrane Mg^{2+} transporter. *Biochem J*. 2007;401(2):505-513.
74. Phelan M, Perrine SP, Brauer M, Faller DV. Sickle erythrocytes, after sickling, regulate the expression of the endothelin-1 gene and protein in human endothelial cells in culture. *J Clin Invest*. 1995;96(2):1145-1151.

How to cite this article: Romero JR, Inostroza-Nieves Y, Pulido-Perez P, et al. Magnesium homeostasis in deoxygenated sickle erythrocytes is modulated by endothelin-1 via Na^+/Mg^{2+} exchange. *The FASEB Journal*. 2022;36:e22638. doi:10.1096/fj.202201339R